JOURNAL OF AGRICULTURAL AND FOOD CHEMISTRY

Metabolic Profiling: A New Tool in the Study of Wood Formation

CAMERON R. MORRIS,[†] JAY T. SCOTT,[†] HOU-MIN CHANG,[†] RONALD R. SEDEROFF,[§] DAVID O'MALLEY,[§] AND JOHN F. KADLA*[,#]

Wood Chemistry and Forest Biotechnology, North Carolina State University, Raleigh, North Carolina 27695, and Biomaterials Chemistry, University of British Columbia, Vancouver, British Columbia, Canada V6T 1Z4

In the realm of plant genomics, metabolic profiling has become a valuable tool with which to assess the effect of genetic and/or environmental factors on plant development. This paper reports the first application of metabolic profiling on differentiating xylem tissue of loblolly pine. A protocol is presented for the analysis of loblolly pine xylem tissue. The effects of sample preparation, extraction, and derivatization on the corresponding metabolite profiles and yields have been investigated and are reported. Gas chromatography−mass spectroscopy has been used to quantify >60 polar and lipophilic metabolites from wood-forming tissue. It was possible to assign chemical structures to approximately half of these compounds. Comparison of six loblolly pine genotypes, three high cellulose (50−52%) and three medium (45−48%) cellulose, showed distinct metabolic profiles. Principal component analysis enabled the assignment of metabolic phenotypes using these large data sets. Metabolic phenotype clustering occurred in which the three high-cellulose genotypes were segregated from the medium-cellulose genotypes. These results demonstrate the use of metabolic profiling for the study of wood-forming tissue and as a tool in functional genomics.

KEYWORDS: Metabolic profiling; principal component analysis (PCA); loblolly pine; xylem tissue; lipid metabolites; polar metabolites

INTRODUCTION

Metabolic profiling is a relatively new but valuable technique being applied in the plant genomic community (*1*). It has its roots in toxicology and blood screening (*2*−*10*), where chemists have long used state-of-the-art chromatography to separate components, followed by mass spectrometry (MS) to identify and quantify them (*3*, *11*, *12*). The main goal of metabolic profiling at that time was to utilize the characteristic features of chromatographic profiles to study the differences between normal and disease states (*13*). To date, when coupled to genomics, the direct use of metabolic profiling offers a quick way to elucidate the function of novel genes. This circumvents uncertainties due to regulation at the levels of transcription, translation, and protein modification.

Metabolic profiles have been defined as multicomponent analyses that produce patterns for a group of metabolically or analytically related metabolites. They are a two-dimensional cross section of a complex multidimensional physiological state delineated by the sample source, chemical processing, and method of analysis. Traditionally defined to be gas chromatography (GC), a profile may be generated by any of a number of instrumental techniques such as gas chromatography−mass spectrometry (GC-MS), liquid chromatography−mass spectrometry (LC-MS), liquid chromatography−nuclear magnetic resonance spectroscopy (LC-NMR), or NMR (*14*−*16*).

A distinction must be made between screening and profiling analyses. In screening, or multiple-metabolite analysis, several compounds are measured, sometimes simultaneously, but in all situations the amounts of these metabolites are compared to the reference ranges in which they are normally found. The concentration of each metabolite is to be considered as a single variable and used in the diagnosis of disease or the evaluation of the state-of-health based on the clinically determined relevance of that particular metabolite. In metabolic profiling, however, the absolute values of particular metabolites are not a major concern; rather, the relative relationship of these metabolites to one another is an equally important consideration (*17*). Another major difference between typical multicomponent analysis and metabolic profiling is that in the profile, the various metabolites are usually metabolically or chemically related. The metabolic profile usually arises from a single analytical procedure, which imposes limitations on the chemical types of metabolites that can be determined in a given analysis. That is, profiles may be obtained for steroids, organic acids, peptides, etc., but not usually mixtures of these different kinds of metabolites. In addition, the profile, which utilizes information from all substances in the sample, those being known as well

* Corresponding author [telephone (604) 827-5254; fax (604) 822-9104; e-mail john.kadla@ubc.ca].
[†] Wood Chemistry.
[§] Forest Biotechnology.
[#] University of British Columbia.

10.1021/jf034688l CCC: $27.50
Published on Web 02/21/2004

as unknown, makes it more able to serve in distinguishing metabolic differences as the results of analyses are studied.

An adoption of the technique of metabolic profiling of plant tissue using GC-MS was first introduced by Sauter, in which the profiling technique was used to study the effect of herbicide treatments on barely leaves (*18*). Recently, Fiehn et al. developed a protocol to study *Arabidopsis thaliana* leaf tissue (*19*). The profiling procedure involves a methanol and chloroform extraction of the plant tissue, followed by phase separation into polar and nonpolar phases. The corresponding phases was methoxylated and trimethylsilylated for the analysis of total fatty acids, fatty alcohols, sterols, and aliphatics, as well as hydroxyamino acids, amino acids, sugars, sugar alcohols, organic monophosphates, (poly)amines, and aromatic acids (*17*). Using GC-MS analysis of the extracts, >300 metabolites were quantified, with 15 of them being uncommon to plants (*20*).

Because softwoods deviated from hardwoods and agricultural crop plant species 350 million years ago, methods need to be established to determine the function of pine genes. As a result, metabolic profiles will provide a key link between plants with unusual processing properties and the identification of the specific genes responsible for those properties. Such profiles from plants can be altered by chemical treatments, environmental changes, genetic engineering, and mutations in unknown genes, all of which provide information on the fundamental questions about the biochemistry of wood fiber formation.

In this paper, we present a protocol for the analysis of loblolly pine xylem tissue. We discuss the effect of sample preparation, extraction, and derivatization on the corresponding metabolite profiles and yields. Also, a data-mining tool, known as principal component analysis (PCA), is applied to the data to illustrate its effectiveness in interpreting the large amounts of data created by metabolic profiling. The overall goal of PCA is to reduce the dimensionality of the data set and ascertain new "meaningful underlying variables" known as principal components (*21*).

MATERIALS AND METHODS

Materials. Methanol (CH_3OH), chloroform ($CHCl_3$), pyridine, sulfuric acid (H_2SO_4), ribitol, nonadecanoic acid methyl ester, methoxyamine hydrochloride, *N*-methyl-*N*-(trimethylsilyl) trifluoroacetamide (MSTFA), and anhydrous sodium sulfate (Na_2SO_4) were of analytical reagent grade (Aldrich Chemical Co.) and used as received.

Methods. *Sampling Procedure.* Samples were collected during the height of wood formation (between May and June). Xylem tissue was obtained from loblolly pine (*Pinus taeda* L.) by cutting away a small window of bark and phloem, typically 4 in. × 8 in., followed by rapid scraping of the xylem tissue into a prechilled sterile centrifuge tube. The tissue was then immediately immersed in liquid nitrogen and transferred to a dry ice chest for transport to the laboratory. NOTE: Once the tree bark has been scored, the trees defense mechanisms will be triggered and the metabolites present will begin to change; therefore, it is imperative that the tissue be collected as quickly as possible and, moreover, that consistent collection times be maintained during the course of repetitive sampling. Generally, the entire process takes ~30 s to collect enough tissue and place the samples in liquid nitrogen once the bark is removed. At the laboratory, the samples were placed in a −80 °C freezer for storage.

Metabolite Extraction and Analysis. Metabolite analysis of xylem tissue was performed using a modified protocol of Fiehn et al. (*19*). Specifically, 300 ± 30 mg of frozen (−80 °C) xylem tissue was ground into a fine powder prior to extraction. Three grinding methods were used: a coffee bean grinder (Gloria Jean's Gourmet Coffee's, model 202), amalgamator (Zenith, model Z14), and a pestle and mortar. Throughout the grinding procedures care was taken to ensure the samples remained frozen.

The ground tissue (300 ± 30 mg) was mixed with 1.4 mL of 100% CH_3OH and vortexed for 10 s to stop any enzymatic activity. Two internal standards were added, 100 μL of ribitol solution (10 mg/mL H_2O) and 100 μL of nonadecanoic acid methyl ester (10 mg/mL $CHCl_3$). A 100-μL aliquot of water was added, the mixture was vortexed, and the tissue was extracted by shaking the mixture for 30 min at 70 °C. The sample was then centrifuged for 3 min at 14000*g*. The supernatant was removed and diluted with 1.4 mL of H_2O in a second centrifuge tube, vortexed, and set aside. The remaining centrifugate was further extracted for 10 min at 37 °C with 2 mL of $CHCl_3$. The mixture was centrifuged at 14000*g* for 3 min, and the supernatant was transferred to the methanol−water extract. The combined extracts were vortexed and centrifuged at 4000*g* for 15 min.

The polar (upper) phase and the lipid (lower) phase of the combined extract were separated into two 7-mL glass vials. Care was taken not to transfer any of the lipid phase over with the polar phase. Both the polar and lipid phase solutions were filtered into 7-mL vials using a 3-mL syringe and a 0.2-μm syringe filter. The polar phase was dried in a speed vac concentrator overnight at 25 °C.

The dried polar phase was dissolved in 100 μL of methoxyamine hydrochloride (20 mg/mL pyridine) and shaken for 90 min at 30 °C. Two hundred microliters of MSTFA was then added, and the solution was shaken for 30 min at 37 °C and then left standing for 2 h at 25 °C. The mixture was then diluted with 200 μL of pyridine, vortexed, and directly injected (2 μL) onto the GC and/or GC-MS.

The lipid phase was transmethylated prior to GC-MS analysis. Accordingly, a 700-μL aliquot of the lipid phase was place into a 10-mL round-bottom flask. To the flask was added 900 μL of $CHCl_3$ and 1 mL of CH_3OH containing 3% v/v H_2SO_4. The reaction was refluxed for 4 h. The reaction was then extracted two times with water (4 mL) and centrifuged at 4000*g* to promote phase separation, and the water phase was removed. The remaining $CHCl_3$ phase was dried over anhydrous Na_2SO_4 and concentrated under reduced pressure to ~80 μL. The acidic protons were derivatized with 10 μL of MSTFA in 10 μL of pyridine for 30 min at 37 °C. After the 30-min derivatization, the sample was injected (2 μL) onto the GC for metabolite quantification and onto the GC-MS for metabolite identification.

The GC system consisted of a Hewlett-Packard 6890 GC-FID, which was controlled by ChemStation. GC analyses were conducted using a 25 m × 0.2 mm J&W Scientific Inc. DB-1 column. The injection temperature was set to 230 °C, the interface temperature was set to 200 °C, and the ion source was set to 250 °C. Helium flow was 1 mL min^{-1}. After a 5-min solvent delay at 70 °C, the oven temperature was increased at 5 °C min^{-1} to 310 °C. The oven was then held isocratic for 1 min and cooled to 70 °C. A threshold cutoff for metabolite analysis was set at 2% of the area of the internal standard. The optimized protocol was repeated five times on the same xylem tissue (number of repetitions limited due to the available xylem tissue). The standard deviation for relative peak areas of various peaks is as follows for the following retention times: 27.95 (0.001461), 29.04 (0.0245324), 31.07 (0.0280746), and 42.73 (0.068925).

The GC-MS system consisted of a ThermoFinnigan TraceGC and PolarisQ ion trap mass spectrometer. The system was controlled by Xcalibur software (version 1.3). The column and method used for analyzing metabolites on the GC-MS system were the same as mentioned previously for the GC method. Mass spectra were recorded from *m*/*z* 50 to 650 at 0.58 s $scan^{-1}$ with an electron ionization of 70 eV.

Lipid Metabolites. Propanoic acid, 2-[(trimethylsilyl)oxy]-, trimethylsilyl ester (**L1**), MW = 234; MS *m*/*z* (rel int) 219 (M − 15, 8), 191 (36), 147 (100), 117 (22), 73 (64).

1-Tetradecyl trimethylsilyl ether (**L6**) MW = 286; MS *m*/*z* (rel int) 271 (M − 15, 100), 103 (20), 75 (55), 73 (25).

Hexadecanoic acid, methyl ester (**L7**), MW = 270; MS *m*/*z* (rel int) 270 (M^+, 30), 227 (51), 199 (41.85), 185 (40), 171 (50), 157 (36), 143 (79), 129 (35), 101 (46), 87 (69), 74 (50), 55 (100).

1,2-Benzenedicarboxylic acid, dibutyl ester (**L8**), MW = 278; MS *m*/*z* (rel int) 278 (M^+, 1), 223 (6), 205 (7), 149 (100), 121 (4), 79 (3).

Hexadecanoic acid, trimethylsilyl ester (**L11**), MW = 328; MS *m*/*z* (rel int) 328 (M^+, 9), 313 (77), 201 (13), 185 (14), 145 (10), 131 (36), 129 (50), 117 (100), 75 (80), 73 (63).

9,12-Octadecadienoic acid, methyl ester (9*E*,12*E*) (**L13**), MW = 294;

MS *m/z* (rel int) 294 (M^+, 4), 262 (14), 164 (15), 150 (11), 135 (20), 109 (15), 96 (25), 95 (30), 81 (77), 79 (80), 67 (100).

9-Octadecenoic acid, methyl ester (**L14**), MW = 296; MS *m/z* (rel int) 296 (M^+, 8), 264 (29), 222 (17), 180 (20), 138 (21), 123 (20), 111 (27), 97 (45), 95 (55), 81 (60), 67 (68), 55 (100).

Hexadecanoic acid, 2-[(trimethylsilyl)oxy]methyl ester (**L15**), MW = 358; MS *m/z* (rel int) 343 (M − 15, 56), 299 (100), 207 (9), 159 (18), 111 (32), 103 (30), 97 (61), 89 (45), 73 (81), 69 (32), 57 (31).

1-Octadecyl trimethylsilyl ether (**L16**) MW = 342; MS *m/z* (rel int) 327 (M − 15, 100), 227 (3), 207 (4), 139 (5), 125 (13), 111 (31), 97 (43), 83 (24), 75 (46), 73 (23), 57 (27).

1-Octadecanoic acid, trimethylsilyl ester (**L19**), MW = 356; MS *m/z* (rel int) 356 (M^+, 15), 341 (92), 313 (16), 297 (15), 257 (19), 201 (26), 145 (17), 132 (30), 129 (68), 117 (90), 75 (100), 73 (72).

1-Phenanthrenecarboxylic acid, 1,2,3,4,4a,9,10,10a-octahydro-1,4a-dimethyl-7-(1-methylethyl)-, methyl ester (**L22**), MW = 314; MS *m/z* (rel int) 314 (M^+,5), 299 (12), 240 (15), 239 (100), 207 (12), 197 (10), 141 (9).

1-Phenanthrenecarboxylic acid, 1,2,3,4,4a,9,10,10a-octahydro-1,4a-dimethyl-7-(1-methylethyl)-, trimethylsilyl ester (**L23**), MW = 372; MS *m/z* (rel int) 372 (M^+, 5), 357 (7), 255 (9), 240 (20), 239 (100), 173 (6), 143 (5), 73 (10).

Bis(2-ethylhexyl) phthalate (**L28**), MW = 390; MS *m/z* (rel int) 279 (M − 111, 11), 167 (52), 149 (100), 71 (5), 57 (7).

Polar Metabolites. Butanedioic acid, [(trimethylsilyl)oxy]-, bis-(trimethylsilyl) ester, (**P1**) MW = 350; MS *m/z* (rel int) 351(M + 1, 14), 335 (15), 263 (19), 245 (17), 233 (24), 189 (17), 149 (75), 147-(63), 133(15), 73(100),

Butanoic acid, 4-[bis(trimethylsilyl)amino]-, trimethylsilyl ester (**P2**), MW = 319; MS *m/z* (rel int) 304 (M − 15, 40), 246 (5), 216 (25), 174 (100), 147 (42), 100 (13), 73 (62).

1-Cyclohexene-4-d-1-carboxylic acid, 3,4,5-tris[(trimethylsilyl)oxy]-, trimethyl silyl ester (**P4**), MW = 462; MS *m/z* (rel int) 462 (M^+, 3), 372 (7), 357 (8), 282 (17), 254 (19), 204 (100), 189 (17), 147 (25), 73 (85).

1,2,3-Propanetricarboxylic acid, 2-[(trimethylsilyl)oxy]-, tris(trimethylsilyl) ester (**P5**), MW = 480; MS *m/z* (rel int) 465 (M − 15, 4), 375 (14), 363 (13), 347 (25), 305 (7), 273 (100), 257 (34), 217 (42), 147 (82), 73 (80).

Cyclohexanecarboxylic acid, 1,3,4,5-tetrakis[(trimethylsilyl)oxy]-, trimethylsilyl ester (**P11**), MW = 552; MS *m/z* (rel int) 553 (M + 1, 13), 537 (11), 419 (8), 345 (100), 334 (6), 255 (66), 204 (9), 191 (11), 147 (25), 73 (66).

D-Fructose-C-d, 1,3,4,5,6-pentakis-O-(trimethylsilyl)- (**P12**), MW = 569; MS *m/z* (rel int) 570 (M + 1, 14), 480 (14), 364 (10), 307 (20), 277 (10), 217 (100), 205 (2), 147 (10), 103 (14), 73 (50).

D-Glucose, 2,3,4,5,6-pentakis-*O*-(trimethylsilyl)- (**P14**), MW = 569; MS *m/z* (rel int) 570 (M + 1, 32), 480 (27), 319 (100), 229 (12), 217 (32), 205 (11), 157 (43), 147 (21), 129 (53), 73 (80).

Inositol, 1-*O*-methyl-2,3,4,5,6-pentakis-*O*-(trimethylsilyl)- (**P16**), MW = 554; MS *m/z* (rel int) 555 (M + 1, 2), 433 (10), 318 (27), 305 (47), 260 (72), 247 (11), 217 (43), 191 (25), 159 (11), 147 (34), 133 (17), 73 (100).

β-D-Glucopyranose, 1,2,3,4,6-pentakis-*O*-(trimethylsilyl)- (**P17**), MW = 540; MS *m/z* (rel int) 539 (M − 1, 2), 435 (14), 361 (18), 243 (5), 217 (26), 204 (100), 191 (48), 147 (12), 129 (8), 73 (69).

Inositol, 1,2,3,4,5,6-hexakis-*O*-(trimethylsilyl)- (**P18**), MW = 612; MS *m/z* (rel int) 613 (M + 1, 4), 507 (8), 432 (12), 318 (56), 305 (100), 265 (33), 217 (94), 191 (45), 147 (36), 129 (20), 1013 (13), 73 (100).

Sucrose, octakis-*O*-(trimethylsilyl)- (**P19**), MW = 918; MS *m/z* (rel int) 451 (M − 466, 1), 437 (19), 361 (100), 271 (13), 217 (13), 169 (24), 147 (6), 129 (6), 73 (39).

Software. Principal component analysis (PCA) was carried out in SAS JMP 4.04.

RESULTS AND DISCUSSION

Variation in Xylem Tissue Grinding Methods and Grinding Times. The grinding of xylem tissue is an important step in the extraction of metabolites. Three methods of tissue grinding were used: pestle and mortar, amalgamator, and a coffee bean grinder with dry ice. The effect of grinding time (1, 2, 5, and 10 min) on metabolite yield was evaluated using the standard extraction and derivatization protocol.

For each of the three grinding methods, it was noted that 1 min of grinding did not sufficiently pulverize the xylem tissue, with grinding times of ≥2 min being required to produce finely ground powders. However, the 1 and 2 min grinding times gave very similar polar phase metabolite results. This was in stark contrast to the level of metabolites obtained from the lipid phase. Two minutes of grinding time produced twice as many metabolites as were obtained from grinding the xylem tissue for only 1 min. Grinding the xylem tissue for >2 min showed no increase in the number of metabolites for both the polar and lipid phases. This is likely due to the fact that 2 min of grinding is sufficient to completely pulverize the tissue and enable the liberation of both the polar and lipid metabolites. Any increase in the duration of mechanical action may serve only to destroy sensitive and unstable metabolites and lead to a decrease in metabolite yields. In fact, the tissue ground for 5 and 10 min showed a decrease in the number of metabolites seen in the lipid phase, despite the fact that the tissue samples were refrozen every 20 s to ensure they remained frozen. Moreover, all three methods exhibited nearly identical results provided that the tissue samples remained frozen during the grinding procedure.

The results obtained indicate that (i) tissue grinding for 2 min provides the optimal yield in metabolites from xylem tissue and (ii) the method of tissue grinding does not greatly affect metabolite yield. It must be stressed that although it is important to accurately weigh the tissue prior to grinding, if not careful, preweighing the tissue for the amalgamator or pestle and mortar methods can lead to the tissue thawing out, allowing the continuous function of the enzymes within the xylem tissue. Therefore, the method employing the coffee grinder, which utilizes dry ice during the grinding process, is preferred. It enables not only the grinding of all of the tissue at one time but also the temperature to be easily maintained at −80 °C. This method permits the finely ground xylem to never increase in temperature and undergo any adverse changes. As needed, the xylem powder can be easily and quickly transferred into a frozen tarred vial and weighed for the extraction process, and the remaining tissue can be placed back into the −80 °C freezer.

Table 1. Extraction Time Matrix for Polar and Lipid Phase Metabolite Extractions[a]

	xylem tissue sample						
	1	2	3	4	5	6	7
polar phase extraction time (min)	5	15	30	60	30	30	30
lipid phase extraction time (min)	5	5	5	5	10	30	60

[a] The initial polar phase extractions were conducted holding the lipid phase extraction constant (samples 1–4). Once an optimum polar phase extraction time of 30 min was achieved, the lipid phase extraction was varied by holding the polar phase extraction constant (samples 5–7).

Variation in Extraction Time. The second variable examined in the profiling protocol was the extraction time. As seen in **Table 1**, several extraction times for both the polar and lipid phases were examined, and the effect of extraction time on the appearance/abundance of metabolites was monitored. The polar phase extraction was analyzed by first holding the lipid phase extraction time constant at 5 min. Results from the polar phase extractions for the 5-, 15-, and 30-min time periods, found in **Figure 1**, presented very similar chromatograms, which indicates that the same numbers of metabolites were released for these

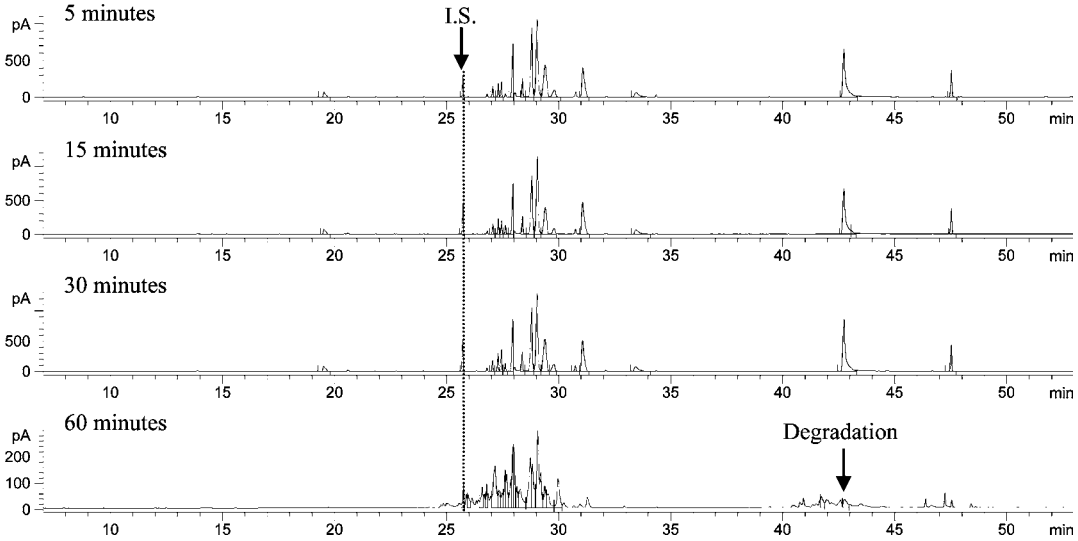

Figure 1. GC chromatograms of polar phase metabolites extracted using various extraction times: 5, 15, 30, and 60 min. Included is the internal standard peak (ribitol) as reference. (All tissues were ground for 2 min at −80 °C prior to extraction.)

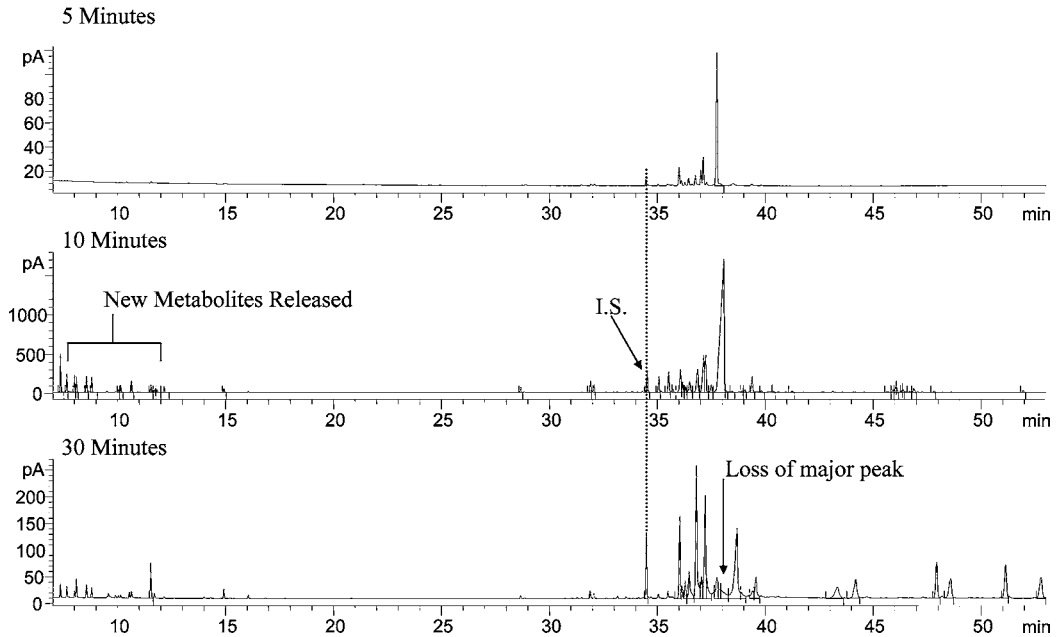

Figure 2. GC chromatograms of lipid phase metabolites extracted using various extraction times: 5, 10, 30, and 60 min. Included is the internal standard peak (nonadecanoic acid methyl ester) as reference. (Lipid phase extractions were made by holding the polar phase extraction time constant at 30 min.)

Table 2. Relative Concentrations of Random Metabolites for Various Polar Phase Extraction Times

polar extraction time (min)	$A_{27.95}/A_{I.S.}$	$A_{29.04}/A_{I.S.}$	$A_{31.07}/A_{I.S.}$	$A_{42.73}/A_{I.S.}$
5	1.96	4.57	2.49	4.52
15	1.97	4.70	2.76	4.15
30	3.33	8.02	4.03	7.46
60	*a*	*a*	*a*	*a*

[a] Due to the presence of apparent decomposition products, the relative concentrations of these metabolites were not determined.

extraction time periods. From a comparison of the relative concentrations between metabolite levels in each chromatogram, **Table 2** shows a difference among the three extraction times: an increase in extraction time has a direct relationship with the concentration of metabolites. However, a change in the profile of metabolites was observed when the extraction time was increased to 60 min. The concentration of metabolites decreased and new metabolites appeared, thus indicating metabolite decomposition or instability under these conditions. Thus, from these results a polar phase extraction time of 30 min appears to produce a maximum amount of polar metabolites in the shortest period of time.

The effect of extraction time for the lipid phase was analyzed by maintaining a constant polar phase extraction time of 30 min. The lipid phase extraction time was varied over the range of 5−60 min. Analogous to the polar phase, **Figure 2** shows that the extraction time had a dramatic effect on the levels of metabolites detected by GC. A 5-min lipid extraction was enough time to release metabolites; however, compared to the 10-min lipid phase extraction there were fewer metabolites released at lower concentrations. As extraction time was increased to 30 min, little change in lipid metabolite levels occurred, except for the loss of a major peak present in previous extraction times. Again at 60 min (data not shown), a substantial decrease in metabolite levels accompanied by an increase in the total number of metabolites observed occurred, analogous

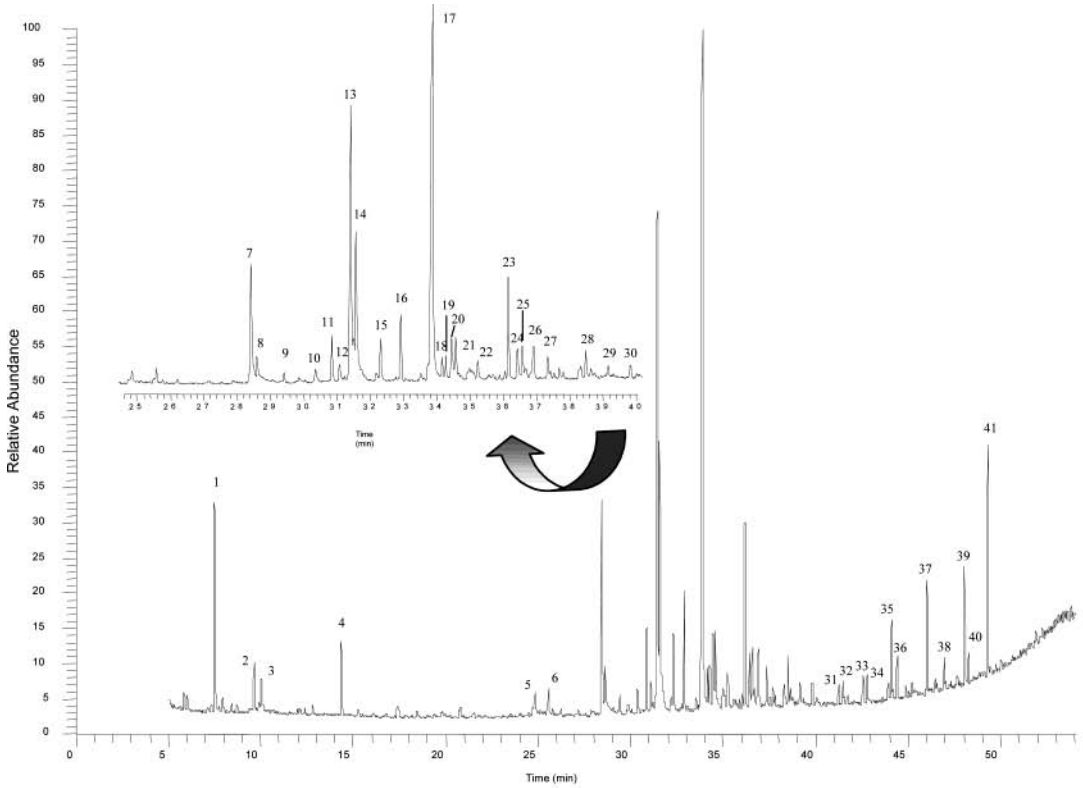

Peak Number	Compound Name	Retention Time	Peak Number	Compound Name	Retention Time
L1	Propanoic acid, 2-[(trimethylsilyl) oxy]-, trimethylsilyl ester	7.50	L22	1-Phenanthrenecarboxylic acid, 1,2,3,4,4a,9,10,10a-octahydro-1,4a-dimethyl-7-(1-methylethyl)-, methyl ester	35.23
L2	Unknown	9.63	L23	1-Phenanthrenecarboxylic acid, 1,2,3,4,4a,9,10,10a-octahydro-1,4a-dimethyl-7-(1-methylethyl)-, trimethylsilyl ester	36.16
L3	Unknown	10.03	L24	Unknown	36.42
L4	Glycerol	14.35	L25	Unknown	36.57
L5	Unknown	24.84	L26	Unknown	36.90
L6	1-Tetradecyl trimethylsilyl ether	25.58	L27	Unknown	37.34
L7	Hexadecanoic acid, methyl ester	28.42	L28	Bis (2-ethylhexyl) phthalate	38.48
L8	Benzenedicarboxylic acid, dibutyl ester	28.59	L29	Unknown	39.16
L9	Unknown	29.41	L30	Unknown	39.82
L10	Unknown	30.35	L31	Unknown	41.22
L11	Hexadecanoic acid, trimethylsilyl ester	30.85	L32	Unknown	41.49
L12	Unknown	31.08	L33	Unknown	42.54
L13	9,12-Octadecadienoic acid, methyl ester	31.42	L34	Unknown	42.77
L14	9-Octadecenoic acid, methyl ester	31.57	L35	Unknown	44.07
L15	Hexadecanoic acid, 2-[(trimethylsilyl)oxy]-methyl ester	32.31	L36	Unknown	44.42
L16	1-Octadecyl trimethylsilyl ether	32.92	L37	Unknown	46.02
L17	Internal Standard- nonadecanoic acid methyl ester	33.89	L38	Unknown	46.95
L18	Unknown	34.17	L39	Unknown	48.06
L19	1-Octadecanoic acid, trimethylsilyl ester	34.27	L40	Unknown	48.24
L20	Unknown	34.44	L41	Unknown	49.30
L21	Unknown	34.57			

Figure 3. Metabolite profile of the lipid phase metabolites obtained from the xylem tissue of wood-forming loblolly pine. Included is a list of identified and unknown metabolites and the corresponding GC retention times.

to that observed for the polar phase. **Scheme 1** summarizes the optimal conditions for the isolation of polar and lipid metabolites.

Variation in Derivatization Time. Once the appropriate extraction times were determined, it was decided to look at the length of derivatization time to ensure that the metabolites of the xylem tissue were being completely derivatized. To study the effects of derivatization time, four derivatization times were chosen and observed for any effects in the number or relative concentration of polar phase metabolites from the xylem tissue. Also, two model compounds (arabinose and caffeate), metabolites identified through mass spectra, were taken and run under identical derivatization conditions to determine the efficacy of derivatization.

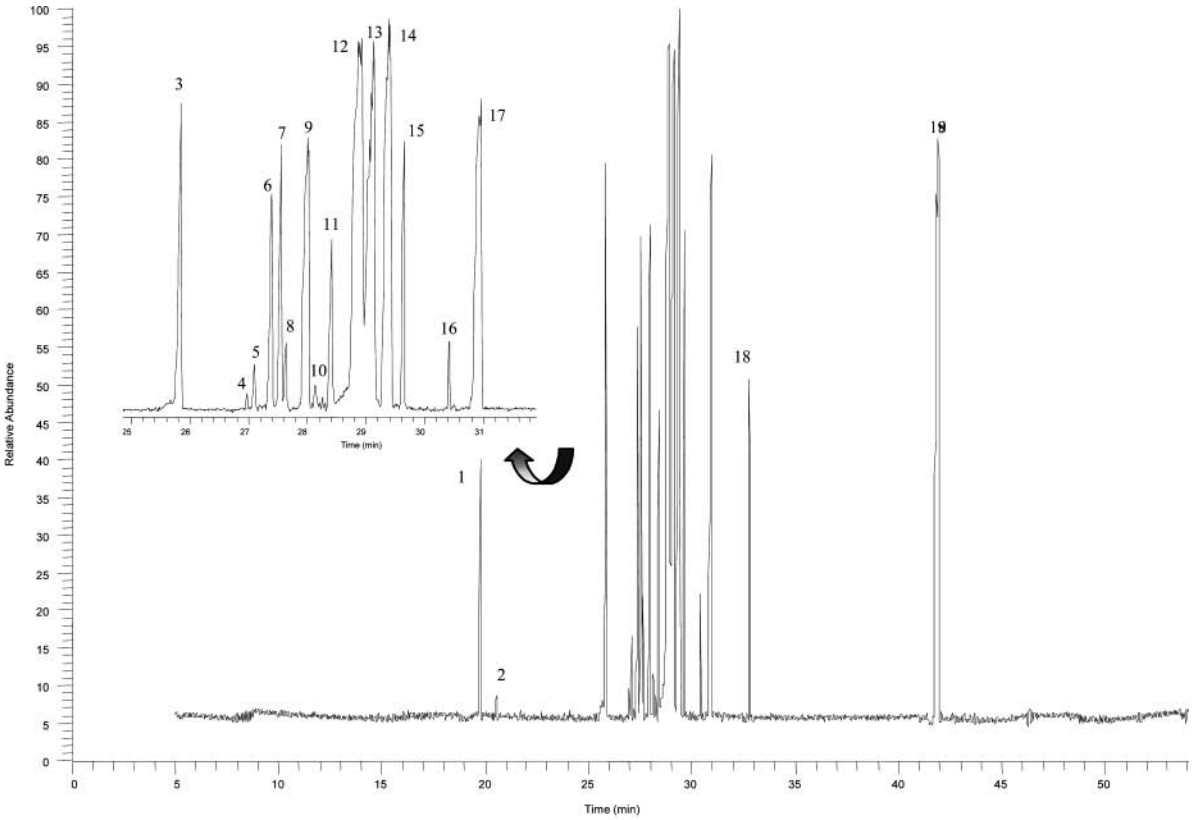

Peak Number	Compound Name	Retention Time	Peak Number	Compound Name	Retention Time
P1	Butanedioic acid, [(trimethylsilyl)oxy]-, bis(trimethylsilyl) ester	19.77	P11	Cyclohexanecarboxylic acid, 1,3,4,5-tetrakis[(trimethylsilyl) oxy]-, trimethylsilyl ester	28.41
P2	Butanoic acid, 4-[bis(trimethylsilyl) amino]-, trimethylsilyl ester	20.56	P12	D-Fructose- 1,3,4,5,6-pentakis-O-(trimethylsilyl)-	28.92
P3	Internal Standard- D-Ribitol-1,2,3,4,5-pentakis-O-(trimethylsilyl)-	25.66	P13	unknown	29.14
P4	1-Cyclohexene-1-carboxylic acid, 3,4,5-tris[(trimethylsilyl)oxy]-trimethyl silyl ester	26.98	P14	D-Glucose, 2,3,4,5,6-pentakis-O-(trimethylsilyl)-	29.38
P5	1,2,3-Propanetricarboxylic acid, 2-[(trimethylsilyl)oxy]-,tris(trimethylsilyl) ester	27.11	P15	unknown	29.65
P6	Unknown	27.40	P16	Inositol, 1-O-methyl-2,3,4,5,6-pentakis-O-(trimethylsilyl	30.41
P7	Unknown	27.56	P17	β-D-Glucopyranose, 1,2,3,4,6-pentakis-O-(trimethylsilyl)-	30.95
P8	Unknown	27.64	P18	Inositol, 1,2,3,4,5,6-hexakis-O-(trimethylsilyl)-	32.79
P9	Unknown	28.00	P19	Sucrose, octakis-O-(trimethylsilyl)-	41.91
P10	Unknown	28.13			

Figure 4. Metabolite profile of the polar phase metabolites obtained from the xylem tissue of wood-forming loblolly pine. Included is a list of identified and unknown metabolites and the corresponding GC retention times—13 of the 19 polar phase metabolites detected have been identified using GC-MS.

Arabinose and caffeate were derivatized individually, as well as in a combined mixture to simulate the derivatization process. Results from the series of tests revealed that a derivatization time of >2 h was sufficient to achieve quantitative derivatization of the individual metabolites or the mixture of metabolites. Similar results were found when the polar phase derivatization was performed on xylem tissue, wherein a maximum in relative concentrations area was observed at between 2.5 and 3.5 h of reaction time.

Metabolic Profiling of Loblolly Pine Xylem Tissue. Figures 3 and **4** show metabolite profiles for the lipid and polar phases obtained from xylem tissue of loblolly pine. It can be seen that a large number of metabolites are observed, and although a majority of them have been identified, several remain unknown. Identification of these unknown metabolites is currently underway. However, the power of metabolic profiling is not in the identification of all metabolites present, but rather in the identification of only those responsible for an observed phenotypic change or difference. We are using metabolic profiling to study genotypic differences in naturally occurring trees with observed differences in phenotype, for example, cellulose content.

Due to the large amounts of data generated by metabolic

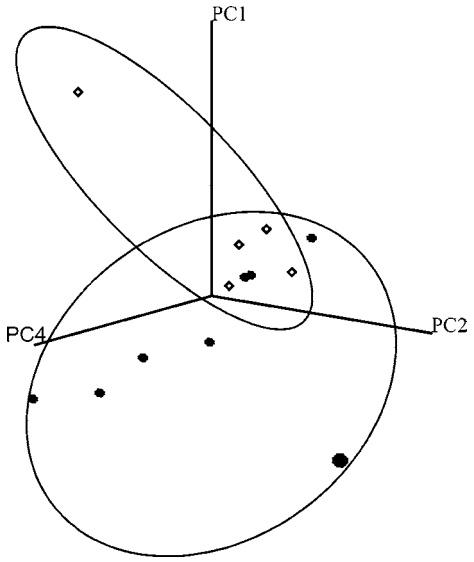

Figure 5. Metabolic phenotype clustering of the polar metabolites after PCA. The data set includes 13 samples representing two groups of separate families. Principal components 1, 2, and 4 contain 74% of the "total information content derived from metabolite variances" (*17*).

Scheme 1. Metabolite Isolation Protocol

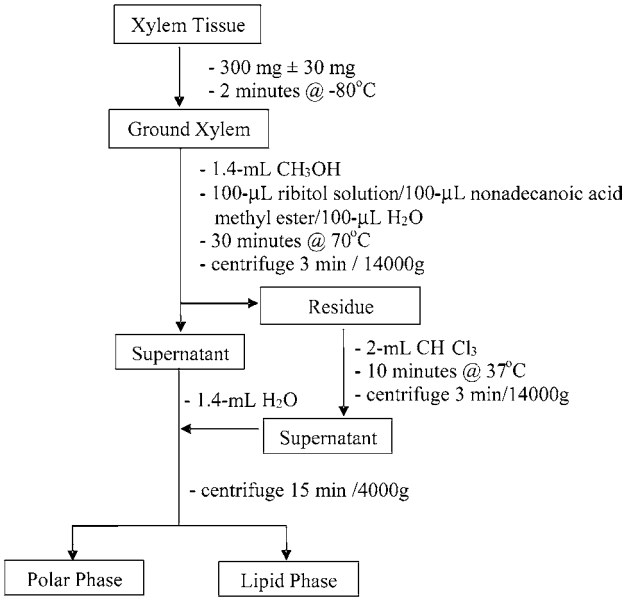

profiles, it is very difficult to interpret the meaning of the enormous amount of chromatographic information. However, PCA is a useful tool that is used to categorize large amounts of data. To exhibit the utility of PCA with the metabolic profiling of xylem tissue, this statistical analysis was applied to xylem tissue collected from 13 trees involved in a breeding program at North Carolina State University that exhibit extreme phenotypic differences in cellulose content. Metabolic profiling in combination with PCA in this study is used to (1) separate the samples into metabolic phenotypic clusters as seen in **Figure 5** and (2) indicate the influence that the metabolites have on the clustering results, which is shown in **Figure 6**.

Figure 5 illustrates the phenotypic cluster created by PCA from the SAS JMP 4.04 software. In this statistical representation, principal components 1, 2, and 4 are used to express 74% of the information compiled from the polar metabolites of 13 individual trees that have been shown to have different levels of alpha cellulose content. The clusters presented are not as

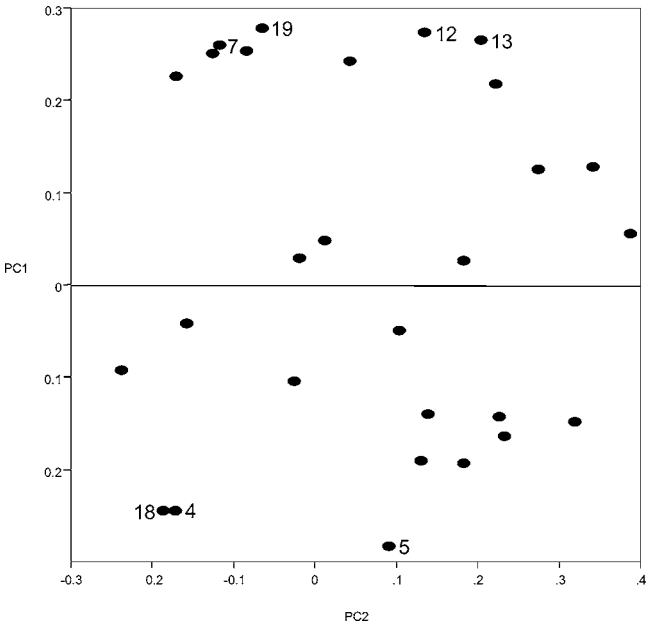

Figure 6. Impact of individual polar metabolites on metabolite clustering. Metabolites farther away from zero have a greater impact on the linear combination that is used to calculate the principal component vector. The labeled metabolites, which are farther from zero, are responsible for the phenotypic differences seen between the two families of trees: 4 = shikimic acid; 5 = citric acid; 7 = unknown; 12 and 13 = D-fructose; 18 = ononitol; 19 = glucopyranose.

tight as one might expect; however, this could be due to the fact that the trees are grown on plots of land in a seed orchard and not a controlled environment, such as a greenhouse. Due to this fact microenvironmental variations are introduced: that is, changes in soil conditions across the plot, temperature gradients, and slopes on the land, which affect groundwater flow, can contribute to variation in the presence of metabolites or metabolite concentration, and which could be responsible for the larger phenotypic clusters.

Plotting principal component 1 versus principal component 2 in **Figure 6** provides the relationship between individual metabolites and clusters formed in **Figure 5**. This graph shows how each individual polar metabolite is utilized in the calculation of the principal component. Metabolites farther away from zero have a greater influence on the calculation of the principal component and those closer to zero have less influence on the calculation. Therefore, the metabolites found farther from the point of zero for principal component 1 are responsible for the phenotypic differences seen between the trees containing high (50−52%) and medium (45−48%) alpha cellulose contents.

The developed protocol shows that a wide range of metabolites, both polar and lipophilic, can be obtained from wood specific xylem tissue. Metabolites that play a major role in wood production have found, for example, shikimic acid, which is a precursor to the lignin biosynthesis pathway, and citric acid, which is an intermediate of the citric acid cycle that generates ATP and also severs as a major source of building blocks for the biosynthesis of amino acids. When coupled to PCA, metabolic profiling can be used to display phenotypic differences as well as the metabolites responsible for those differences.

LITERATURE CITED

(1) Trethewey, R. N.; Krotzky, A. J.; Willmitzer, L. Metabolic profiling: a Rosetta Stone for genomics? *Curr. Opin. Plant Biol.* **1999**, *2*, 83−85.

(2) Garner, R. C.; Leong, D. Pushing the accelerator—speeding up drug research with accelerator mass spectrometry. *Nucl. Instrum. Methods Phys. Res. Sect. B: Beam Interact. Mater. Atoms* **2000**, *172*, 892−898.
(3) Holland, J. F.; Leary, J. J.; Sweeley, C. C. Advanced Instrumentation and Strategies For Metabolic Profiling. *J. Chromatogr.* **1986**, *379*, 3−26.
(4) Hong, J. F.; Baldwin, R. P. Profiling clinically important metabolites in human urine by capillary electrophoresis and electrochemical detection. *J. Capillary Electrophoresis* **1997**, *4*, 65−71.
(5) Lim, H. K.; Stellingweif, S.; Sisenwine, S.; Chan, K. W. Rapid drug metabolite profiling using fast liquid chromatography, automated multiple-stage mass spectrometry and receptor-binding. *J. Chromatogr. A* **1999**, *831*, 227−241.
(6) Matsumoto, I.; Kuhara, T. A new chemical diagnostic method for inborn errors of metabolism by mass spectrometry—Rapid, practical, and simultaneous urinary metabolites analysis. *Mass Spectrom. Rev.* **1996**, *15*, 43−57.
(7) Ning, C.; Kuhara, T.; Inoue, Y.; Zhang, C. H.; Matsumoto, M.; Shinka, T.; Furumoto, T.; Yokota, K.; Matsumoto, I. Gas chromatographic mass spectrometric metabolic profiling of patients with fatal infantile mitochondrial myopathy with de Toni-Fanconi-Debre syndrome. *Acta Paediatr. Jpn.* **1996**, *38*, 661−666.
(8) Rashed, M. S.; Bucknall, M. P.; Little, D.; Awad, A.; Jacob, M.; Alamoudi, M.; Alwattar, M.; Ozand, P. T. Screening blood spots for inborn errors of metabolism by electrospray tandem mass spectrometry with a microplate batch process and a computer algorithm for automated flagging of abnormal profiles. *Clin. Chem.* **1997**, *43*, 1129−1141.
(9) Tayek, J. A.; Bergner, E. A.; Lee, W. P. Correction of Glucose Carbon Recycling For the Determination of True Hepatic Glucose-Production (Hgp) Rates By 1-13C-Glucose. *Clin. Res.* **1990**, *38*, A570−A570.
(10) Toshimitsu, N. Metabolic Profiling with Gas Chromatography−Mass Spectroscopy and Its Application to Clinical Medicine. *J. Chromatogr.* **1986**, *379*, 313−345.
(11) Adams, R. F. Determination of amino acid profiles in biological samples by gas chromatography. *J. Chromatogr.* **1974**, *95*, 189−212.
(12) Toshimitsu, N. Metabolic Profiling with Gas-Chromatography−Mass Spectroscopy and Its Applications to Clinical Medicine. *J. Chromatogr.* **1986**, *379*, 313−345.
(13) Niwa, T. Metabolic Profiling with Gas Chromatography−Mass Spectrometry and its Applications to Clinical Medicine. *J. Chromatogr.* **1986**, *379*, 313−345.
(14) Fraser, P. D.; Elisabete, M.; Pinto, S.; Holloway, D. E.; Bramley, P. M. Application of High-Performance Liquid Chromatography with Photodiode Array Detection to the Metabolic Profiling of Plant Isoprenoids. *Plant J.* **2000**, *24*, 551−558.
(15) Glassbrook, N.; Beecher, C.; Ryals, J. Metabolic profiling on the right path. *Nat. Biotechnol.* **2000**, *18*, 1142−1143.
(16) Le Gall, G.; Colquhoun, I. J.; Davis, A. L.; Collins, G. J.; Verhoeyen, M. E. Metabolite Profiling of Tomato (*Lycopersicon esculentum*) Using 1H NMR Spectroscopy as a Tool to Detect Potential Unintended Effects Following a Genetic Modification. *J. Agric. Food Chem.* **2003**, *51*, 2447−2456.
(17) Fiehn, O.; Kopka, J.; Dormann, P.; Altmann, T.; Trethewey, R. N.; Willmitzer, L. Metabolite profiling for plant functional genomics. *Nat. Biotechnol.* **2000**, *18*, 1157−1161.
(18) Sauter, H.; Lauer, M.; Fritsch, H. Metabolic Profiling of Plants—a New Diagnostic Technique. *ACS Symp. Ser.* **1991**, *No. 443*, 288−299.
(19) Fiehn, O. Protocol for Plant Leaf Metabolite Profiling; 2000; http://www.mpimp-golm.mpg.de/fiehn/blatt-protokoll-e.html.
(20) Fiehn, O.; Kopka, J.; Tretheway, R.; Willmitzer, L. Identification of Uncommon Plant Metabolites Based on the Calculation of Elemental Compostions Using Gas Chromatography and Quadrupole Mass Spectrometry. *Anal. Chem.* **2000**, *72*, 3573−3580.
(21) Praat, P. httP://www/fon.hum.uva.nl/praat/manual/Principal_component_ analysis.html

Received for review June 26, 2003. Revised manuscript received January 12, 2004. Accepted January 13, 2004. Financial support from USDA-IFAFS (Grant 2001-52104-11224) is gratefully acknowledged.

JF034688L